Supporting Information

Hyperpolarized NMR metabolomics at natural ^{13}C abundance

Arnab Dey[a], Benoît Charrier[a], Estelle Martineau[a,b], Catherine Deborde[c,d], Elodie Gandriau[a], Annick Moing[c,d], Daniel Jacob[c,d], Dmitry Eshchenko[e1], Marc Schnell[e1], Roberto Melzi[e2], Dennis Kurzbach[f], Morgan Ceillier[g], Quentin Chappuis[g], Samuel F. Cousin[g], James G. Kempf[e3], Sami Jannin[g], Jean-Nicolas Dumez[a], Patrick Giraudeau*[a]

---

[a] Université de Nantes, CNRS, CEISAM UMR 6230, F-44000 Nantes, France
*E-mail: patrick.giraudeau@univ-nantes.fr
[b] SpectroMaitrise, CAPACITES SAS, Nantes, France.
[c] INRAE, Université de Bordeaux, UMR Biologie du Fruit et Pathologie, Centre INRAE de Nouvelle Aquitaine-Bordeaux, F-33140 Villenave d'Ornon, France
[d] Bordeaux Metabolome, MetaboHUB, Centre INRAE de Nouvelle Aquitaine-Bordeaux, F-33140 Villenave d'Ornon, France. INRAE 2018 doi: 10.15454/1.5572412770331912E12
[e] Bruker Biospin, [1] Industriestrasse 26, 8117 Fällanden, Switzerland, [2] Viale V. Lancetti 43, 20158 Milano, Italy, [3] 15 Fortune Dr., Billerica, MA 01821 USA
[f] University of Vienna, Faculty of Chemistry, Institute of Biological Chemistry, Währinger Str. 38, 1090 Vienna, Austria
[g] Université de Lyon, CNRS, Université Claude Bernard Lyon 1, ENS de Lyon, Centre de RMN à Très Hauts Champs (CRMN), FRE 2034, F-69100 Villeurbanne, France.

Table of Contents:

1. Experimental Details

1.1 Chemicals Used

Deuterium oxide (D_2O; 99.9% D), glycerol-d_8 (99% D), deuterium chloride (DCl; 99.9% D) and sodium deuteroxide (NaOD, 40 wt. % in D_2O; 99.5% D) were purchased from Eurisotop (http://www.eurisotop.com). 4-hydroxy-2,2,6,6-tetramethylpiperidine-1-oxyl (4-hydroxy-TEMPO or TEMPOL), sodium 3-trimethylsilylpropionate-d_4 (Na-TSP-d_4; 98% D), disodium ethylene diamine tetraacetate (EDTA.Na_2.$2H_2O$), L-alanine, sodium acetate, sodium pyruvate and sodium [1-^{13}C] acetate (99%, ^{13}C) were obtained from Sigma-Aldrich (www.sigmaaldrich.com). D,L-[1-^{13}C] alanine (99%, ^{13}C) and sodium [1-^{13}C] pyruvate (99%, ^{13}C) were purchased from Cambridge Isotope Laboratories, Inc. (https://www.isotope.com).

1.2 Tomato Extract Preparation for d-DNP

Tomato (*Solanum lycopersicum* L., Sassari cultivar) plants were grown in a greenhouse at UMR Biologie du Fruit et Pathologie, Centre INRAE de Nouvelle Aquitaine-Bordeaux, according to commercial practices. Fruits at two different developmental stages (mature-green and red-ripe) from different plants were harvested and fruit pericarps were sampled and immediately frozen in liquid nitrogen. The frozen samples were cryo-ground (6750 Freezer/Mill, Spex SamplePrep, Metuchen, USA) before freeze-drying. All extracts were prepared from 20 mg of lyophilized powder sample. Polar metabolites were extracted with a series of three ethanol−water solutions at 80 °C following a protocol described previously.[1] Each supernatant solution was dried under vacuum, then solubilized in 200 mM deuterated phosphate buffer solution at apparent pH 6.0 containing 2 mM EDTA.Na_2.$2H_2O$, and pH adjusted by means of a titration unit (BTpH, Bruker, Kalrsruhe, Germany) at apparent pH 6.00+/-0.02 using 1 M NaOD or 1 M DCl. EDTA.Na_2.$2H_2O$ was added to chelate paramagnetic ions and thus to attenuate their paramagnetic effects on the ^{13}C NMR detection of metabolites with carboxylic acid groups such as citrate, malate, fumarate, or various amino-acids. Each pH-adjusted extract was frozen in liquid nitrogen, freeze-dried and stored at -20°C before analysis. A blank sample was also prepared following the same steps as above, but without biological material.

Each frozen extract was dissolved with 2 mM of EDTA.Na_2.$2H_2O$, 20 mM Na-TSP-d_4 (internal reference) in 0.2 mL of a H_2O/D_2O/glycerol-d_8 (1:4:5) glass-forming mixture doped with 50 mM TEMPOL. When ready for use, a resulting single-sample solution (approx. 200 μL), was transferred to the sample holder, for ripening and sample vitrification in the d-DNP polarizer, as described ahead. The solutions were contained within the active volume of radio frequency (RF) coil of the polarizer.

1.3 Standard Metabolite Mixture Preparation

To evaluate the effect of Hellmanex® treatment on lineshape and linewidth, a standard solution containing three metabolites (D,L-[1-^{13}C] alanine, sodium [1-^{13}C] acetate, sodium [1-^{13}C] pyruvate) at a 50 mM concentration each was dissolved with 2 mM of EDTA.Na_2.$2H_2O$, 20 mM Na-TSP-d_4 (internal reference) in 0.5 mL of a H_2O/D_2O/glycerol-d_8 (1:4:5) mixture doped with 50 mM TEMPOL.

To evaluate the repeatability and further optimization of the instrument, a standard solution containing three 50 mM metabolites at natural abundance (L-alanine, sodium acetate, sodium pyruvate), 2 mM of EDTA.Na_2.2H_2O, 20 mM Na-TSP-d_4 (internal reference) was dissolved in 1 mL of a H_2O/D_2O/glycerol-d_8 (1:4:5) mixture doped with 50 mM TEMPOL. Five successive DNP experiments were performed to calculate the coefficient of variation (CV (%)) for ^{13}C signals at natural abundance. For each dissolution experiment, 200 µL of the standard solution were transferred to the sample holder (the same being used for all experiments). All standard solutions were contained within the active volume of the radiofrequency (RF) coil of the polarizer.

1.4 Prototype Bruker d-DNP Polarizer

The prototype Bruker d-DNP Polarizer provides methods (^1H,^{13}C cross-polarization, microwave frequency modulation and gating) and optimal field (7 T) and temperature (1.15 K) for state-of-the-art polarization levels and throughput. It is built on a standard 7T wide-bore magnet and cryostat design, modified to accommodate a variable temperature insert (VTI). The VTI enables DNP at 1.15 K, using *l*-He introduced from a transport dewar (e.g., 100 L) and custom transfer line into a phase separator (PS) near the top of the VTI. From there, a membrane pump (Vacuubrand MD 4 NT) transfers cold *g*-He, whose enthalpy cools the neck, baffles & radiation shields of the VTI, while l-He flows down from the PS and enters the sample space via automated needle valves near the VTI tail. A main pump (Edwards iGx600L) acts on the admitted l-He for final cooling of the sample space, whose temperature setpoint is chosen via feedback-controlled butterfly valve to the pump. The fundamental cyrogenic design is a template for ongoing development of a zero-consumption format.

For DNP itself, microwaves near 197.5 GHz and 125 mW are produced from a synthesizer (8-20 GHz) and 198 GHz amplifier multiplier chain (AMC, 16x frequency), both from Virginia Diodes, Inc. Frequency modulation is programed via the low-frequency source, while microwave gating is achieved via TTL pulses from the Bruker AV NEO NMR console to the AMC. For NMR, the 2-channel console runs Topspin 4 and is coupled to a custom Bruker ^1H,^{13}C probe, with an external (room-*T*) tuning and matching for an overall circuit able to achieve simultaneous nutation frequencies of 50 kHz without arcing.

Dissolution is achieved upon manual coupling of a fluid transfer stick to the sample cup after it has been lifted (~10 cm) to just above the *l*-He level. The stick includes parallel capillaries (1.6 mm ID): an inlet for preheated, pressured D_2O (10 bar, 170 °C) and an outlet to carry hyperpolarized fluid to a 5 mm NMR tube situated in the probe of the solution NMR observation magnet. There, a passive receiver system accepts the turbulent dissolution output, then promotes phase separation and settling during gravity introduction to the NMR tube at ambient temperature and pressure.

1.5 Dissolution Dynamic Nuclear Polarization: experimental parameters

Each DNP solution was kept for 40 min (“ripening interval”) at room temperature before it was vitrified by rapid (<5 s) lowering from room temperature to near 4 K in the sample region of the prototype d-DNP polarizer (Bruker Biospin). The sample space was then sealed and pumped to achieve base temperature (1.18 K) within about 15 min.[2] DNP was performed at 1.18 K and 7.05 T by polarizing

protons using microwave irradiation at $f_{\mu w}$ = 197.7 GHz and $P_{\mu w}$ = 100 mW with a triangular frequency modulation[3] with at bandwidth ($\Delta f_{\mu w}$) of ± 5 MHz and frequency of 10 kHz. Resulting ^{1}H polarization was transferred to ^{13}C by 16 CP contacts of 1.5 ms each at intervals of 40 s, with radiofrequency (RF) powers of 15 W on ^{1}H (using rectangular pulse with constant RF amplitudes of 21 kHz) and 60 W on ^{13}C (using ramped up pulse with linearly increasing RF amplitudes from 16 kHz to 23.2 kHz).[4] Adiabatic half passage pulses (WURST) of 30 W (pulse duration of 175 μs, sweep width of 100 kHz) power were used on both channels before and after the CP contacts (pulse sequence in Figure S1).

After the sixteenth CP contact (*i.e.*, after 11 min), the sample was lifted just above the helium bath, and a dissolution 'stick' was rapidly (<1 s) inserted to the cryostat where it seals to the sample cup. The stick contains a capillary to deliver 5 mL of D_2O (preheated to T = 170 °C at P = 10 bar) to dissolve the sample, and a second capillary to carry this product out of the cryostat and across to the nearby magnet for 400 MHz solution NMR observation (~1.6 m between magnet centres of the d-DNP polarizer and 400 MHz systems). In dissolution steps, we took care to always lift the sample to the same position in the magnetic field of the polarizer and to actuate dissolution at the same temperature. The transfer was driven by helium gas originating at 10 bar passing through both capillaries of the dissolution stick and on to the 400 MHz solution-state NMR spectrometer. A 1.6 mm inner diameter ETFE capillary was used to exit from the polarizer to the solution NMR magnet, and along the way ran through a 0.56 T magnetic tunnel (DNP Instrumentation, https://dnp-instrumentation.com/) and finally injected via a gas-liquid phase separator into a 5 mm NMR tube. The complete dissolution, transfer, and injection took 7.8 s. This is the typical time to fill the 5 mm NMR tube with current apparatus. Longer times detailed with Fig. 3 of the main text reflect additional, empirically determined delays to allow further settling in the before triggered acquisition of the high-resolution, solution-state NMR spectrum.

1.6 Liquid state NMR acquisition parameters

All d-DNP enhanced NMR experiments were recorded at 298 K on a 400 MHz Bruker Avance Neo spectrometer equipped with liquid-N_2 cryogenically cooled probe (5 mm CryoProbe™ Prodigy BBFO with ATMA and Z-gradient from Bruker BioSpin). For the ^{13}C-enriched standard metabolite mixture, ^{13}C spectra were acquired immediately after the described injection of the sample to 5 mm NMR tube. A series of spectra were recorded sequentially with small-angle (5°) pulses preceded by a 1 s delay and followed by a 2.29 s acquisition time using Waltz-16 ^{1}H decoupling (Individual 1D spectra in the series were acquired with a fixed time interval of 3.39 s constituting a pseudo 2D experiment). It was then processed with 0.3 Hz Lorentzian line-broadening, zero filled to 256 k data points, Fourier transformed and manually phase corrected.

The ^{13}C spectra of the standard metabolite mixture at natural abundance and of all the hyperpolarized tomato extracts were recorded after a delay of 12.8 s from dissolution followed by a 90° pulse in a single scan with a 1.7 s acquisition time and Waltz-16 ^{1}H decoupling during acquisition, then processed with Bruker TopSpin (v 4.0.5.0) with a 1 Hz exponential line broadening and zero-filled to 256 k data points. Before data analysis, hyperpolarized ^{13}C spectra of tomato extract were manually phase corrected and baseline corrected using a 3rd degree polynomial in the 50-200 ppm range.

1.7 Extract data processing

Following the phase and global baseline correction with TopSpin, spectral regions of interest, *i.e.* containing resonances of the whole dataset of hyperpolarized ^{13}C spectra from the extracts were processed with NMRProcFlow (v 1.3.12)[5] (http://nmrprocflow.org) for local baseline correction, local realignment and spectral area integration (intelligent and variable sized bucketing) to obtain 40 spectral regions (Figure S3) or "buckets" . Each of the integral values from those buckets was normalized with respect to the Na-TSP-d_4 (internal reference) signal integral at 188.6 ppm and further normalized with respect to the dry weight of the fruit powder used for extraction. The normalized signal integrals were subjected to PCA analysis using the SIMCA software (https://umetrics.com/simca). PCA is the most commonly used multivariate data analysis technique in metabolomics.[6] PCA transforms the multidimensional dataset containing the integral values of all the buckets into a two-dimensional dataset (termed as 1st and 2nd principal components; PC1 and PC2 respectively) to emphasize the variability among samples. Each PC is composed of the linear combination of all the original variables (buckets); PCA is therefore an unsupervised method that does not induce any artificial separation unlike supervised methods. In the PCA analysis, mean centering and unit variance scaling was chosen and the first two PCs were plotted. The PC1 x PC2 plan accounted for 80.5 % of total variation among data points. Mature-green and red-ripe samples were statistically compared for all buckets using Kruskal-Wallis test (with FDR correction for multiple testing) performed with BioStatFlow tool based on R scripts (http://biostatflow.org/).

1.8 Bucket annotation

Bucket annotation resulted in the assignment of 15 metabolite resonances (Table S1): two sugars (fructose and sucrose) and two organic acids (citric and malic acids) crucial for fruit cell growth and ripening and fruit taste, and 11 amino acids (alanine, asparagine, aspartic acid, GABA, glutamic acid, glutamine, isoleucine, leucine, pyroglutamic acid, threonine, valine), among which 13 could be quantified individually and 12 are common with a previous study about fruit of another tomato cultivar performed using ^{1}H-NMR profiling at 500 MHz [6]. Glucose, mannose and choline quantified in the latter study could not be seen here as they do not have quaternary carbons.

The present assignments allowed revealing significantly higher contents (Kruskal-Wallis, $p< 0.05$, Figure S4) in green fruit compared to red fruit for several free amino acids including aspartic acid, asparagine, GABA, leucine and threonine, and malic acid. Sucrose and fructose, citric acid and glutamic acid have higher contents in tomato red-fruit extracts. These trends of metabolic changes during fruit ripening are in clear agreement with previously published data based on ^{1}H-NMR profiling of tomato extract (Supplementary Figure 1 of [7]) or on other analytical strategies (gas chromatography coupled with mass spectrometry [8]) for the major compounds sucrose, fructose, citric, malic and glutamic acids, all crucial for tomato fruit taste (sweetness, acidity and umami flavour, respectively).

2. Procedure of Hellmanex® Treatment

We first prepared an Hellmanex® solution by adding 2% by volume Hellmanex® III solution from Hellma Analytics (https://www.hellma.com/en/laboratory-supplies/cuvettes/hellmanex/) in deionized water. Then, NMR tubes were filled with this solution, and placed in a water bath at 40 °C for 40 min. After that, tubes were emptied and rinsed with deionized water twice. Finally, NMR tubes were dried in an oven at 40 °C overnight. A freshly treated NMR tube was used with each dissolution.

3. Supplementary figures and table

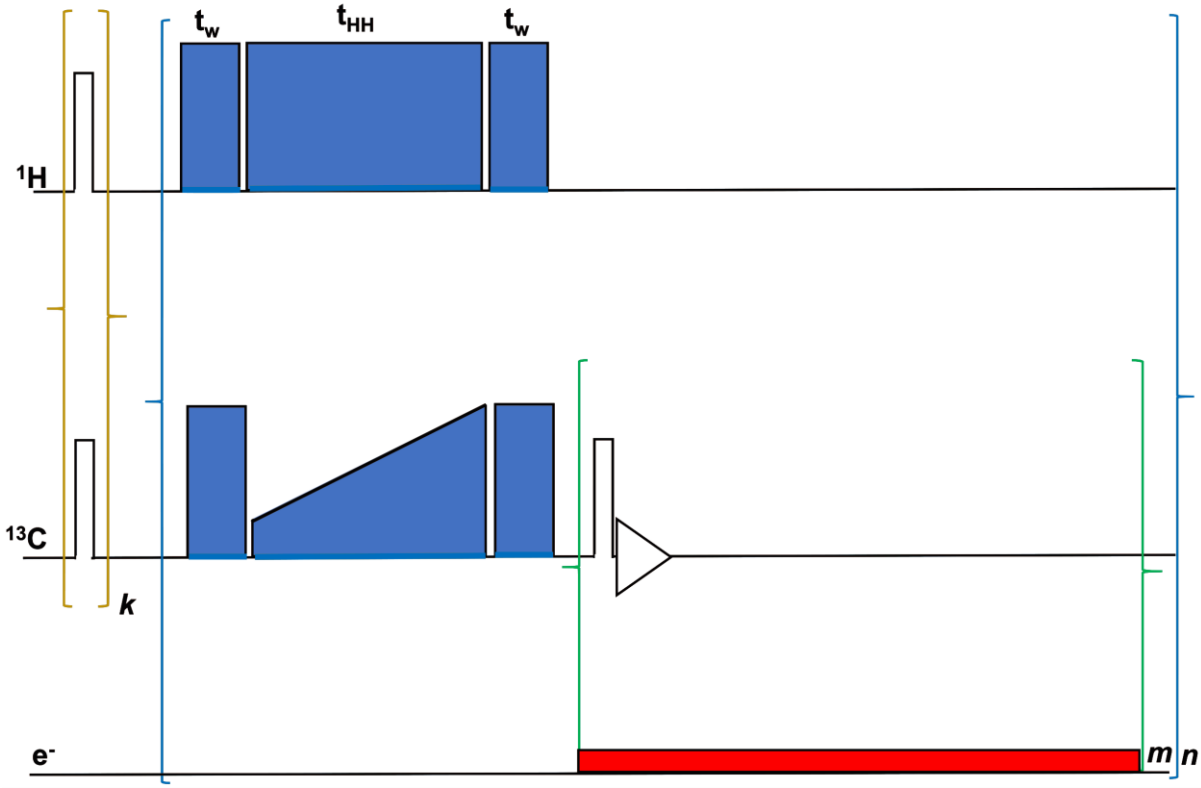

Figure S1: Solid state DNP pulse sequence via cross polarization (CP) for d-DNP. A train (*k*=64) of $\pi/2$ pulses was applied to both RF channels for pre-saturation. Here CP (referred as "blue" blocks) was performed using adiabatic half passage pulses (t_w = 175 µs) to convert longitudinal magnetization to transverse magnetization before the start of the contact pulse (t_{HH} = 1.5 ms) and vice versa after the contact. Contact pulse uses radiofrequency (RF) powers of 15 W on ^1H (using rectangular pulse with constant RF amplitudes of 21 kHz) and 60 W on ^{13}C (using ramped up pulse with linearly increasing RF amplitudes from 16 kHz to 23.2 kHz). In total 16 CP contacts (n=16) were made. For each contact, a sequence of m=4 pulses with low-flip-angle pulse (5°) was applied on ^{13}C channel to monitor the buildup of the polarization from ^1H to ^{13}C. Microwave irradiation was selectively switched on after each CP contact for 40 s (referred as "red" block) to improve DNP polarization efficiency by avoiding the significant contribution of electron spin in nuclear spin relaxation rate.[9]

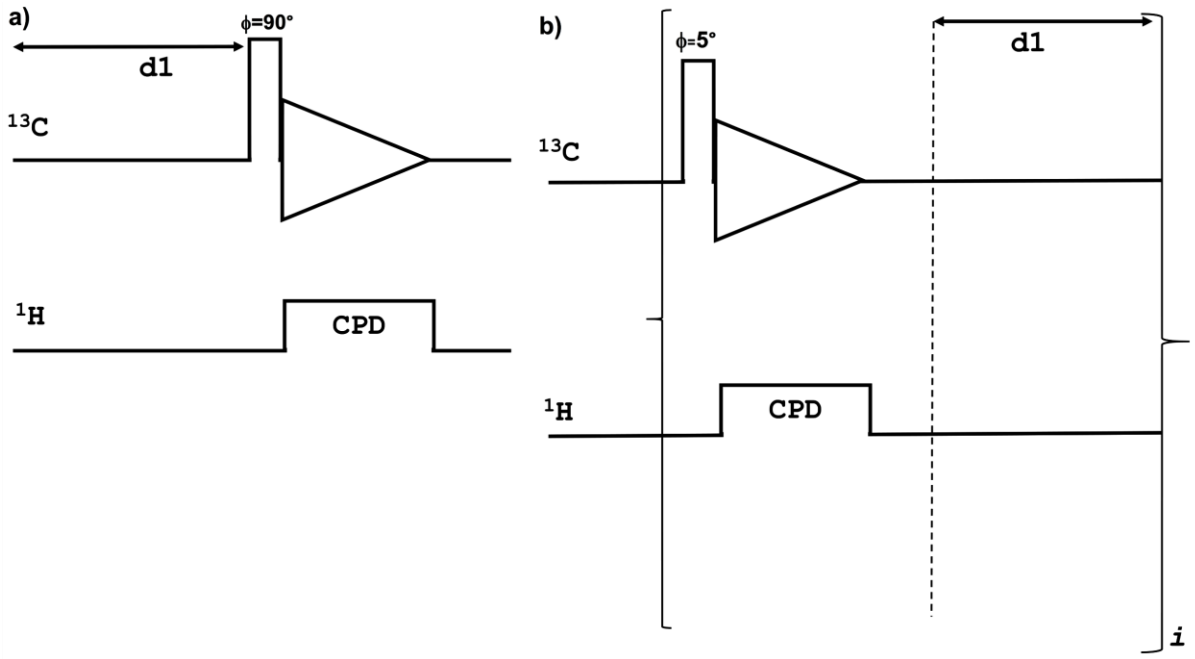

Figure S2: NMR acquisition pulse diagram implemented a) to monitor the repeatability of ^{13}C signal at natural abundance and for the analysis of hyperpolarized tomato extracts; b) to evaluate the effect of Hellmanex® treatment on lineshape and linewidth on ^{13}C-enriched samples. Here *i* is the repetition index which indicates number of hyperpolarized ^{13}C signals acquired sequentially after a fixed delay.

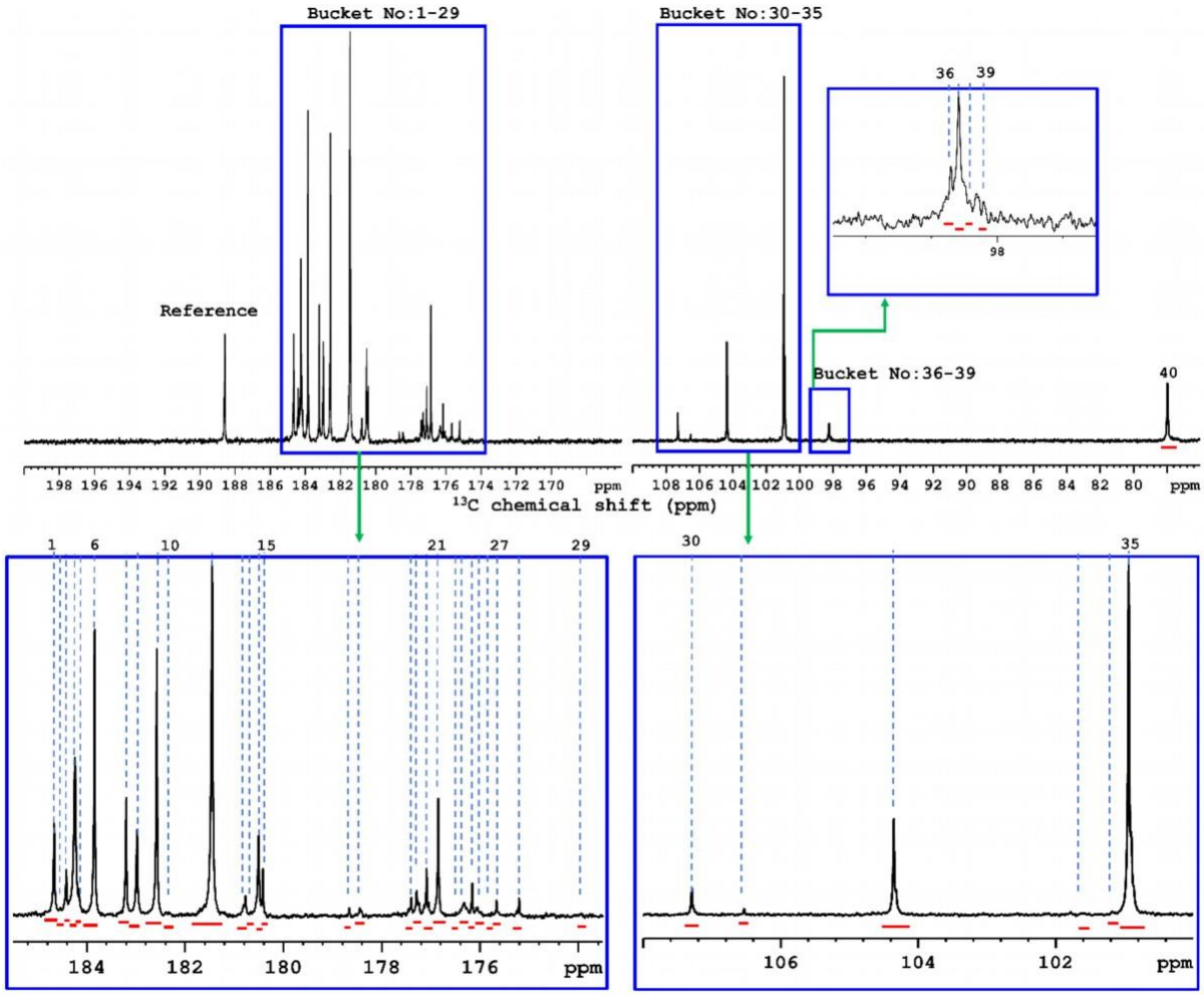

Figure S3: Representative d-DNP enhanced single-scan ^{13}C NMR spectrum of a tomato mature-green fruit extract indicating the 40 spectral regions ("buckets") defined with NMRProcFlow[4] and used for signal integration. The centers of the buckets (see inset) are indicated in blue color and sizes of the buckets are shown as red horizontal lines at the bottom of the spectrum.

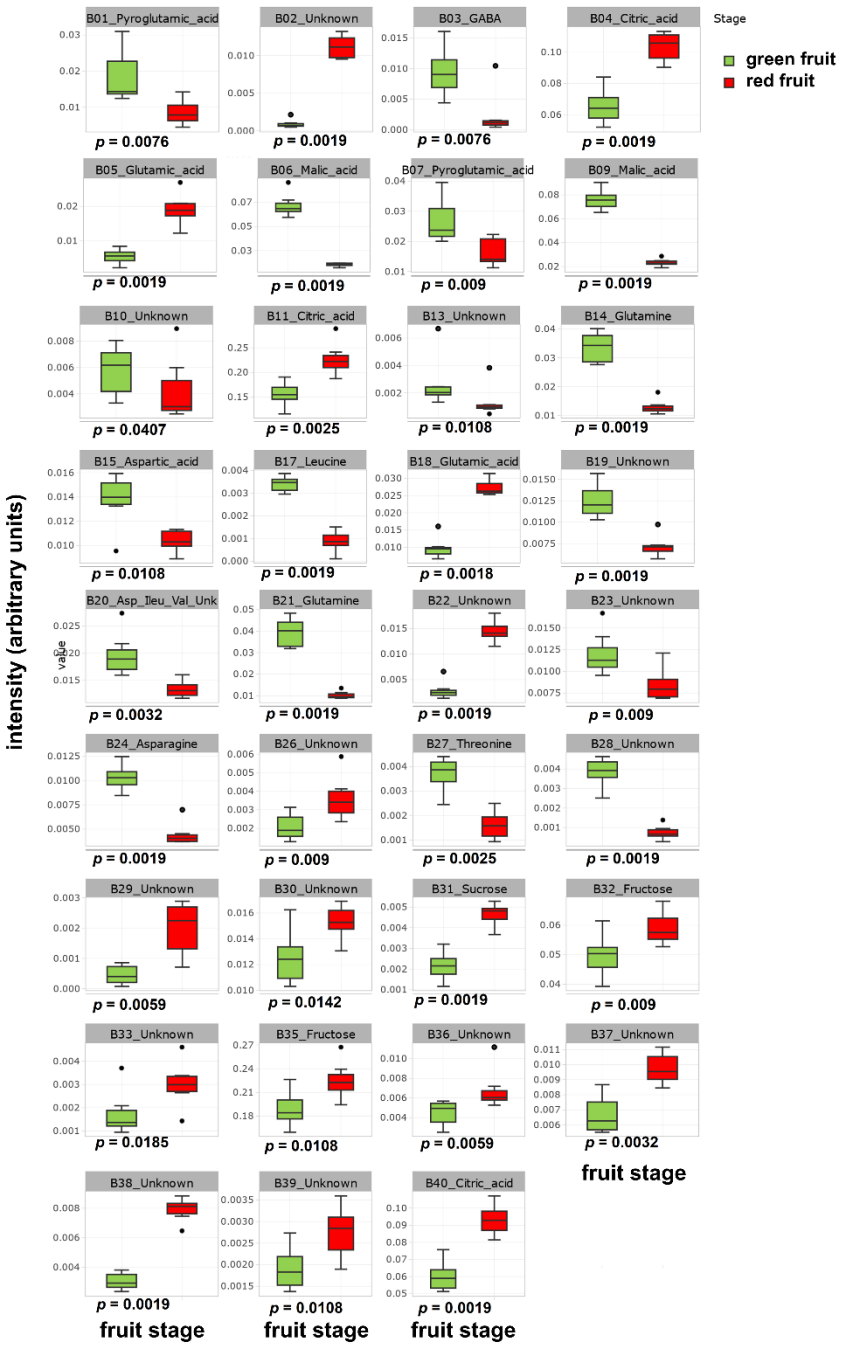

Figure S4: Whisker-plots of 35 discriminant buckets of d-DNP enhanced single-scan ^{13}C NMR spectra of tomato fruit extracts ($p < 0.05$) after Kruskal-Wallis analyses on 40 buckets, and corresponding *p*-values at the bottom of each box plot. Each box shows the interquartile range (IQR) divided by the median, whiskers indicate 1.5 × IQR (n=8) and full circles are outlier samples. Bucket assignments are detailed in Table S1. Asp, aspartic acid; Ileu, isoleucine; Val, valine; Unk, unknown compound.

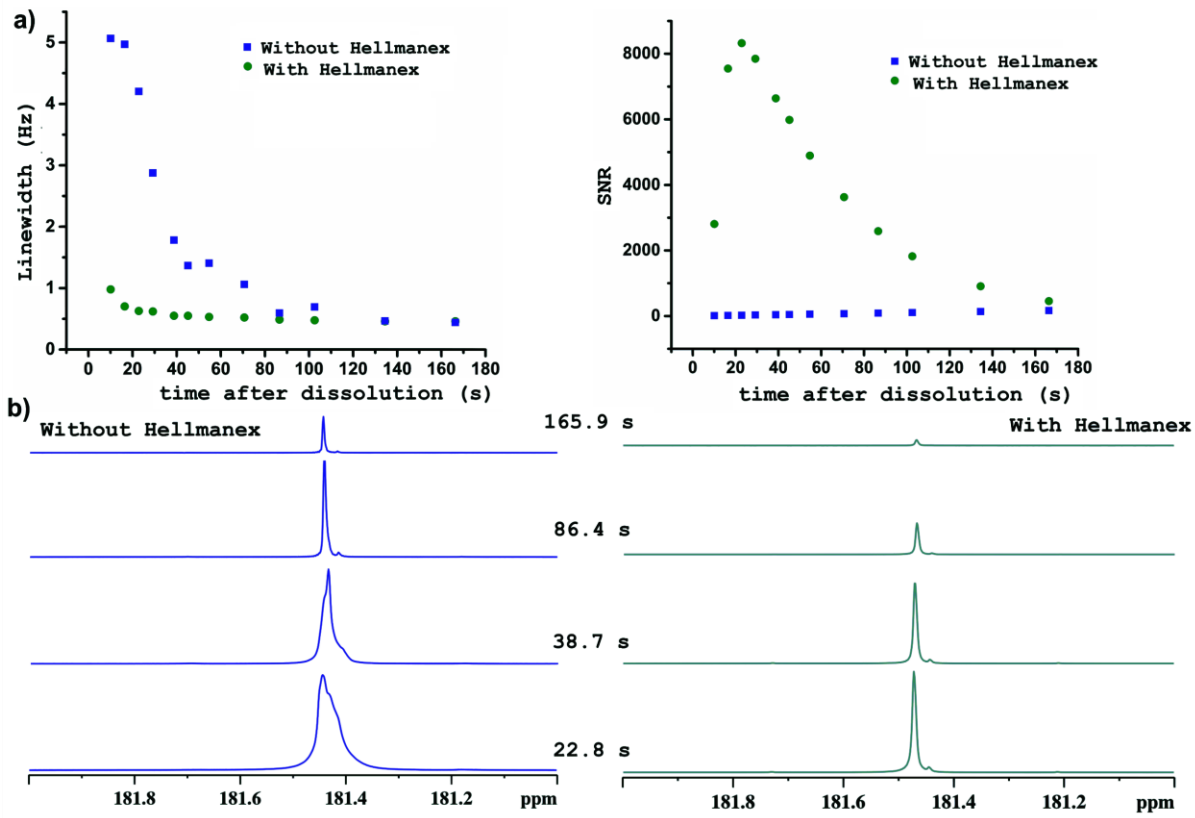

Figure S5: ^{13}C NMR spectra of sodium[1-^{13}C] acetate in a mixture sample of ^{13}C enriched standard metabolites highlighting the ability of Hellmanex® treatment of the NMR tube to improve the lineshape and linewidth. This sample tube treatment results in a significant improvement in ^{13}C sensitivity, since it enables a much shorter post-acquisition delay to reach an optimum SNR. (a) Plot shows the change of linewidth and SNR with the time after dissolution with and without Hellmanex® treatment. (b) Spectra show the change of lineshape at different delays after dissolution with and without Hellmanex® treatment.

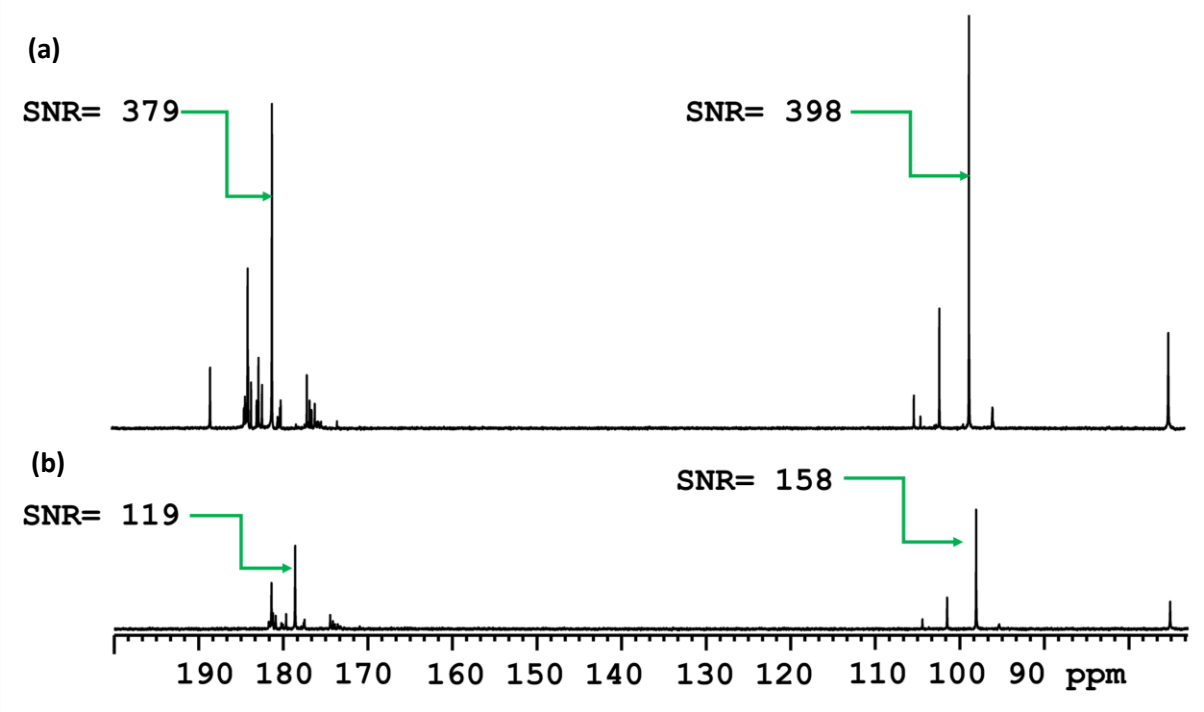

Figure S6: A comparison figure of d-DNP enhanced single-scan ^{13}C NMR spectra of red tomato fruit extract (a) after and (b) before optimization. Spectra obtained (a) at 12.8 s after dissolution, with Hellmanex® treatment and after addition of Na-TSP-d_4; (b) at 22.8 s after dissolution, without Hellmanex® treatment and without addition of Na-TSP-d_4.

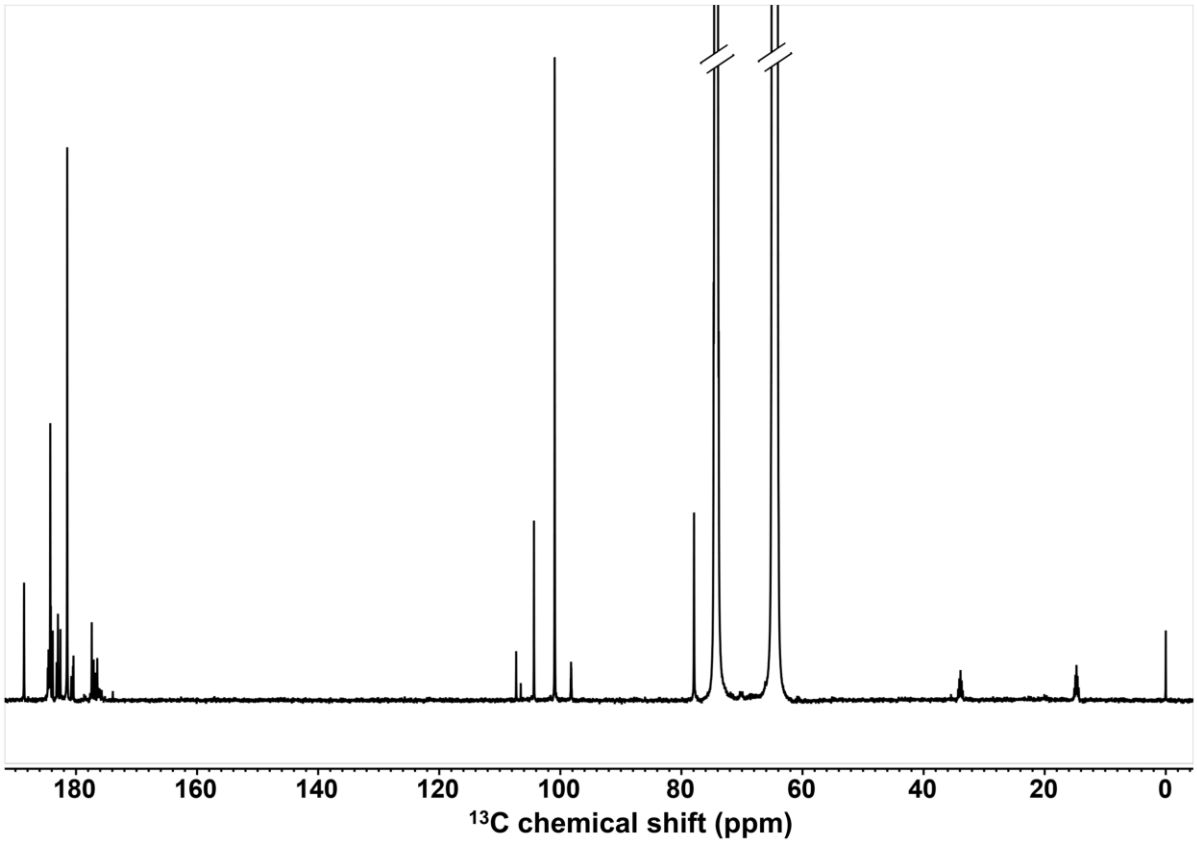

Figure S7: Full chemical shift range d-DNP enhanced singe-scan ^{13}C NMR spectrum of tomato red-fruit extract. Spectrum was calibrated with the ^{13}C signal of Na-TSP-d_4 at 188.6 ppm. Spectrum shows the ^{13}C signal of glycerol-d_8 at 64.6 ppm and 74.3 ppm.

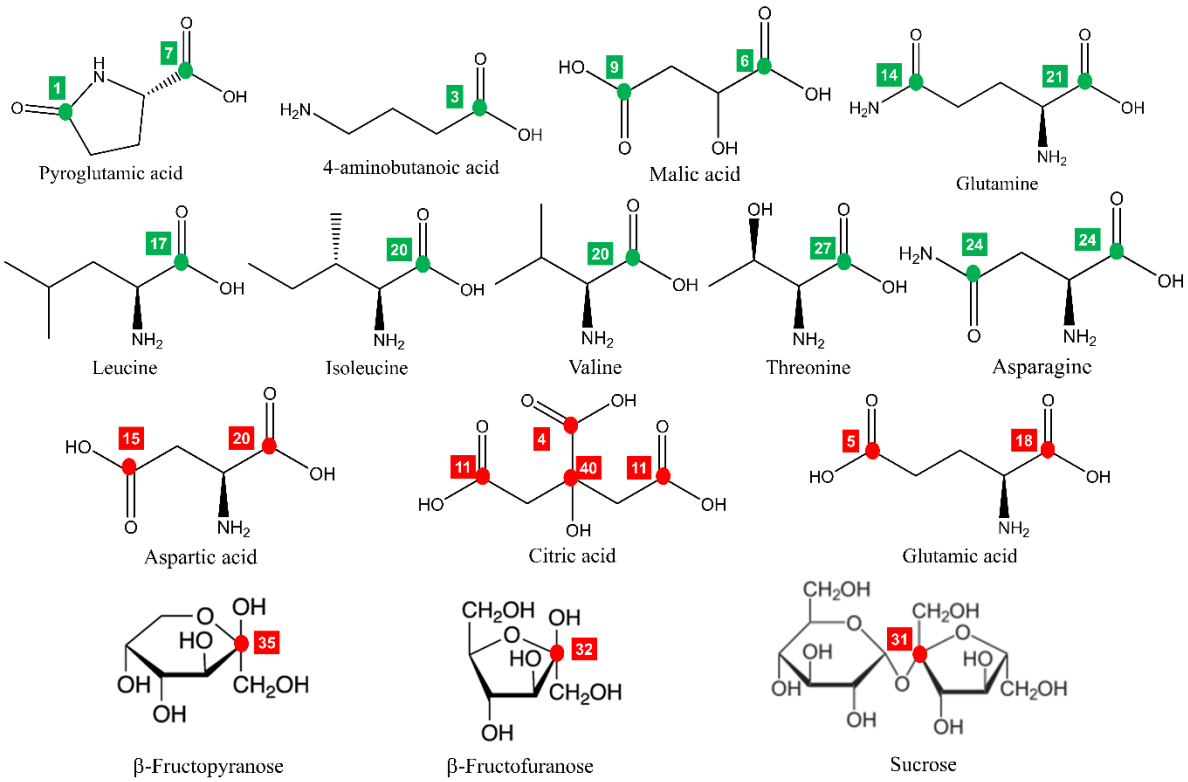

● **Observed resonance of quaternary ^{13}C site of discriminant metabolite of green tomato**

● **Observed resonance of quaternary ^{13}C site of discriminant metabolite of red tomato**

N **Bucket number of discriminant metabolite resonance of green tomato**

N **Bucket number of discriminant metabolite resonance of red tomato**

Figure S8: Chemical structures of discriminant compounds that have been detected in the d-DNP enhanced single-scan ^{13}C NMR spectra of pericarp extracts of tomato fruit at two stages of development. Quaternary Carbon sites (those without directly attached ^{1}H) whose resonances have been detected by d-DNP ^{13}C-NMR are labeled. These correspond to Table S1.

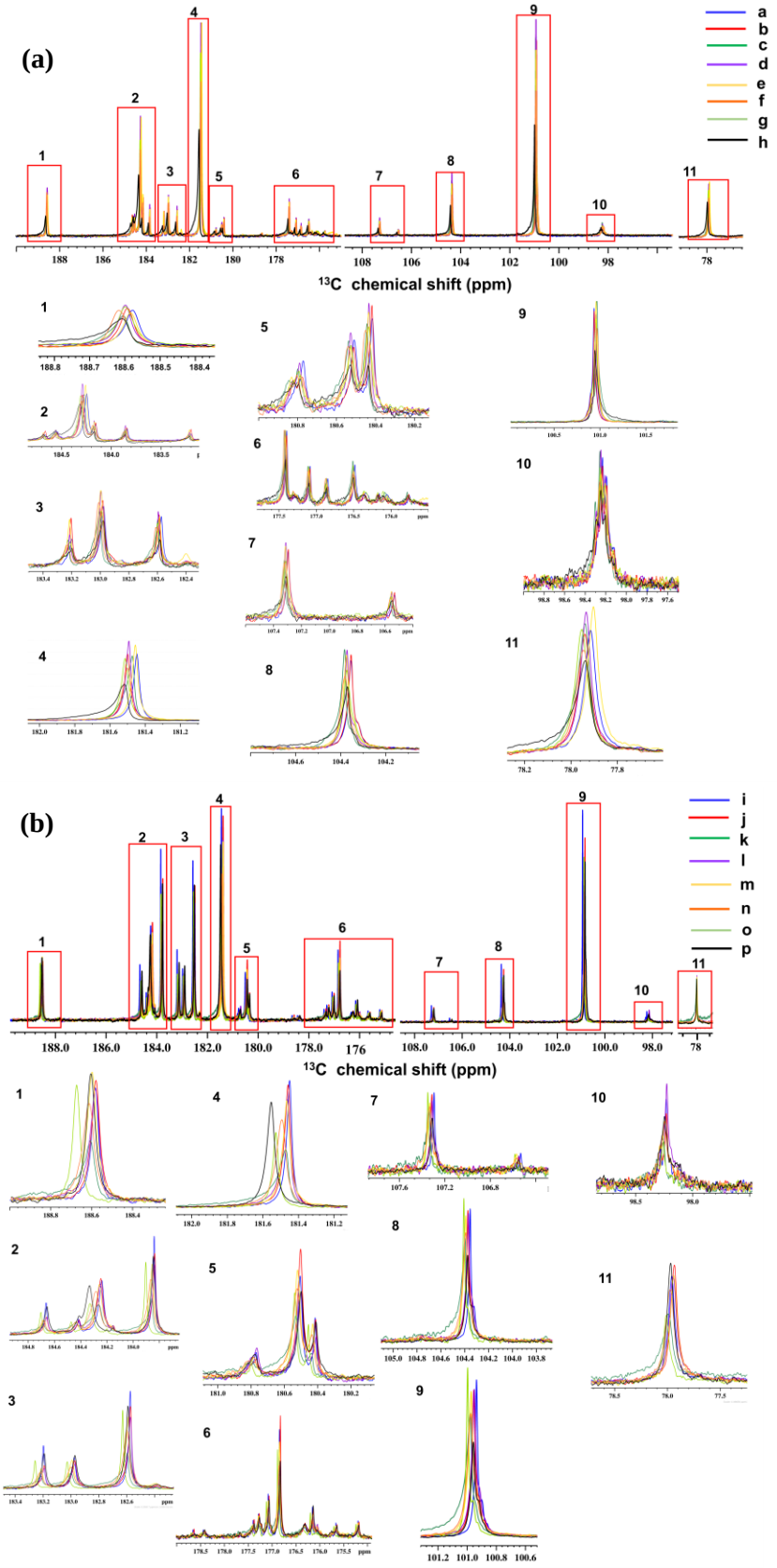

Figure S9: Superimposed plot of d-DNP enhanced single-scan ^{13}C NMR spectra of 16 tomato samples containing (a) 8 red-ripe tomato extracts; (b) 8 mature green tomato extracts. The specific regions of the spectra are magnified (denoted by numbers) and shown at the bottom of each type of extracts.

Table S1: List of compounds and metabolites* detected in the d-DNP enhanced single-scan ^{13}C NMR spectra of pericarp extracts of tomato fruit at two stages of development.

Bucket n°	Bucket name	Metabolite Name	Metabolite ID	MSI level**
1	B184_6681	Pyroglutamic acid	**CHEBI:16010**	2
2	B184_5226	Unknown		4
3	B184_4158	GABA	**CHEBI:16865**	4
4	B184_2680	Citric acid	**CHEBI:30769**	2
5	B184_1184	Glutamic acid	**CHEBI:18237**	2
6	B183_8341	Malic acid	**CHEBI:6650**	2
7	B183_1856	Pyroglutamic acid	**CHEBI:16010**	2
8	B182_9659	EDTA-M	**CHEBI:42191**	1
9	B182_5765	Malic acid	**CHEBI:6650**	2
10	B182_3562	Unknown		4
11	B181_4874	Citric acid	**CHEBI:30769**	2
12	B180_7801	Unknown		4
13	B180_6254	Unknown		4
14	B180_5141	Glutamine	**CHEBI:28300**	2
15	B180_3639	Aspartic acid	**CHEBI:22660**	2
16	B178_6377	Alanine	**CHEBI:16449**	2
17	B178_4050	Leucine	**CHEBI:25017**	2
18	B177_4092	Glutamic acid	**CHEBI:18237**	2
19	B177_2403	Unknown		4
20	B177_0679	Aspartic acid + Isoleucine + Valine + Unknown	**CHEBI:22660 ; CHEBI:24898; CHEBI:27266**	4
21	B176_8418	Glutamine	**CHEBI:28300**	2
22	B176_4765	Unknown		4
23	B176_3178	Unknown		4
24	B176_1517	Asparagine	**CHEBI:22653**	2
25	B176_0067	Unknown		4
26	B175_7589	Unknown		4
27	B175_6368	Threonine	**CHEBI:26986**	2
28	B175_1698	Unknown		4
29	B173_9014	Unknown		4
30	B107_2979	Unknown		4
31	B106_5227	Sucrose	**CHEBI:17992**	3
32	B104_3638	Fructose (β-fructofuranose)	**CHEBI:28757**	2
33	B101_6370	Unknown		4
34	B101_1819	Unknown		4
35	B100_9239	Fructose (β-fructopyranose)	**CHEBI:28757**	2
36	B98_3094	Unknown		4
37	B98_2283	Unknown		4
38	B98_1672	Unknown		4
39	B98_0828	Unknown		4
40	B78_0244	Citric acid	**CHEBI:30769**	2

*The green and red highlighted metabolites refer to the predominant metabolites present in green and red tomato fruit extracts, respectively ($p < 0.05$, Kruskal-Wallis). The metabolite without highlight refers to a non-discriminant metabolite which was present in both tomato extracts ($p >= 0.05$, Kruskal-Wallis). ** MSI status [10]: 1: identified compound; 2: putatively annotated compound; 3: putatively characterized compound classes; 4: unknown compound. *** EDTA-M: Metal-EDTA complexes, M: mainly Ca^{2+}.

References

[1] a) J.-N. Dumez, J. Milani, B. Vuichoud, A. Bornet, J. Lalande-Martin, I. Tea, M. Yon, M. Maucourt, C. Deborde, A. Moing, L. Frydman, G. Bodenhausen, S. Jannin, P. Giraudeau, *The Analyst* **2015**, *140*, 5860-5863; b) C. Bénard, S. Bernillon, B. Biais, S. Osorio, M. Maucourt, P. Ballias, C. Deborde, S. Colombié, C. Cabasson, D. Jacob, G. Vercambre, H. Gautier, D. Rolin, M. Génard, A. R. Fernie, Y. Gibon, A. Moing, *Journal of Experimental Botany* **2015**, *66*, 3391-3404.

[2] E. M. M. Weber, G. Sicoli, H. Vezin, G. Frébourg, D. Abergel, G. Bodenhausen, D. Kurzbach, *Angewandte Chemie International Edition* **2018**, *57*, 5171-5175.

[3] A. Bornet, J. Milani, B. Vuichoud, A. J. Perez Linde, G. Bodenhausen, S. Jannin, *Chemical Physics Letters* **2014**, *602*, 63-67.

[4] A. Bornet, R. Melzi, A. J. Perez Linde, P. Hautle, B. van den Brandt, S. Jannin, G. Bodenhausen, *The Journal of Physical Chemistry Letters* **2012**, *4*, 111-114.

[5] D. Jacob, C. Deborde, M. Lefebvre, M. Maucourt, A. Moing, *Metabolomics* **2017**, *13*.

[6] J. J. Jansen, S. Smit, H. C. J. Hoefsloot, A. K. Smilde, *Phytochemical Analysis* **2010**, *21*, 48-60.

[7] M. Lemaire-Chamley, F. Mounet, C. Deborde, M. Maucourt, D. Jacob, A. Moing, *Metabolites* **2019**, *9*, 93.

[8] G. Oms-Oliu, M. L. A. T. M. Hertog, B. Van de Poel, J. Ampofo-Asiama, A. H. Geeraerd, B. M. Nicolaï, *Postharvest Biology and Technology* **2011**, *62*, 7-16.

[9] A. Bornet, A. Pinon, A. Jhajharia, M. Baudin, X. Ji, L. Emsley, G. Bodenhausen, J. H. Ardenkjaer-Larsen, S. Jannin, *Physical Chemistry Chemical Physics* **2016**, *18*, 30530-30535.

[10] L. W. Sumner, A. Amberg, D. Barrett, M. H. Beale, R. Beger, C. A. Daykin, T. W. M. Fan, O. Fiehn, R. Goodacre, J. L. Griffin, T. Hankemeier, N. Hardy, J. Harnly, R. Higashi, J. Kopka, A. N. Lane, J. C. Lindon, P. Marriott, A. W. Nicholls, M. D. Reily, J. J. Thaden, M. R. Viant, *Metabolomics* **2007**, *3*, 211-221.